# Conformational Effects on the Photoinduced Energy Transfer in a Star-Shaped Pentaporphyrin with Nucleosidic Linkers

Lucia Flamigni,*[a] Anna Maria Talarico,[a] Barbara Ventura,[a] Giancarlo Marconi,[a]
Chloé Sooambar,[b] and Nathalie Solladié*[b]

**Keywords:** Circular dichroism / Energy transfer / Porphyrinoids / Photochemistry / Supramolecular chemistry

The photophysical properties of a pentameric array (**FB-Zn$_4$**) containing peripheral Zn porphyrins and a free-base core, connected by nucleosidic linkers, have been determined and compared with the properties of the model dyad (**FB-Zn**) and of their individual components. The flexibility of the nucleosidic linkers allows the dyad to take two different conformations corresponding to a bent and an almost fully extended form of the linker, which are characterized by a chromophore separation of ca. 2 nm and ca. 3 nm, respectively. Energy transfer from the zinc porphyrin to the free-base porphyrin occurs, in the bent conformation, with a rate of $3.6 \times 10^9$ s$^{-1}$. Conversely, in the extended conformation, the Zn porphyrin decay is unperturbed, which is in good agreement with the expected dipole–dipole (Förster) energy transfer mechanism. In the pentameric array, the Zn porphyrin luminescence is quenched with a rate of $3.6 \times 10^9$ s$^{-1}$ in 15% of the population, whilst the luminescence of the Zn porphyrin is unquenched for ca. 35% of the population. For comparison with the dyad, these two cases are assigned as arrays with a single linkage in a bent configuration and arrays with all linkages in the extended configuration, respectively. However, the most striking feature in the pentaporphyrin is that 50% of the Zn porphyrin excited state population exhibits a fast nonradiative deactivation (rate ca. $10^{10}$ s$^{-1}$) which also involves the free-base porphyrin core to some extent. This behavior is attributed to a strongly interacting conformation with the Zn porphyrins folded over the central free-base porphyrin. The proposed model is supported by CD spectroscopy, complexation experiments with bases, and the reactivity of the excited state towards external quenchers.

## Introduction

Synthesis of multi-porphyrin architectures and determination of their photo properties is the object of intensive research activity.[1] These oligomeric arrays can mimic naturally occurring tetrapyrrolic aggregates that perform key processes in photosynthesis, i.e. light energy collection and charge separation.[2] The study of multi-porphyrin ensembles, in addition to providing basic knowledge in the fields of photochemistry, photophysics and photobiology, can be regarded as potentially informative in the construction of light-operated molecular-level information storage devices, [3] for the conversion of light energy into chemical or electrical energy,[1,4] and for the preparation of materials with novel properties.[5]

The present system, which consists of a pentaporphyrin containing a central free-base porphyrin and four peripheral zinc porphyrins connected via a flexible chiral nucleosidic linker,[6] was studied in order to determine its potential as an antenna system, capable of collecting light energy and conveying it to the energy sink at the central position. The peripheral zinc porphyrin chromophores can absorb light extensively over the full visible spectrum and the energy stored in the first excited singlet state (2.05 eV) could be conveyed to the central free-base porphyrin characterized by a lower lying excited singlet state (1.92 eV). The system can work effectively as an antenna if the absorbed light energy is efficiently conveyed to the central porphyrin and no competitive loss of the absorbed energy occurs. The study of convenient model compounds, **ZnU**, **FBS** and the dyad **FB-Zn**, whose structures are shown in Scheme 1, can help in the elucidation of the fundamental steps in the pentad system **FB-Zn$_4$**, where photophysical behavior could be strongly influenced by the existence of different conformations due to the flexible linkers. Steady state and time-resolved spectroscopic methods were used to quantify the energy transfer process which was postulated previously.[6]

---

[a] Istituto per la Sintesi Organica e Fotoreattivita' (ISOF), CNR,
Via P. Gobetti 101, 40129 Bologna, Italy
E-mail: flamigni@isof.cnr.it
[b] Groupe de Synthèse de Systèmes Porphyriniques, Laboratoire d'Electrochimie et de Chimie Physique du Corps Solide, Université Louis Pasteur et CNRS (UMR 7512), Institut Le Bel,
4 rue Blaise Pascal, 67000 Strasbourg, France
E-mail: nsolladie@chimie.u-strasbg.fr

DOI: 10.1002/ejic.200300918

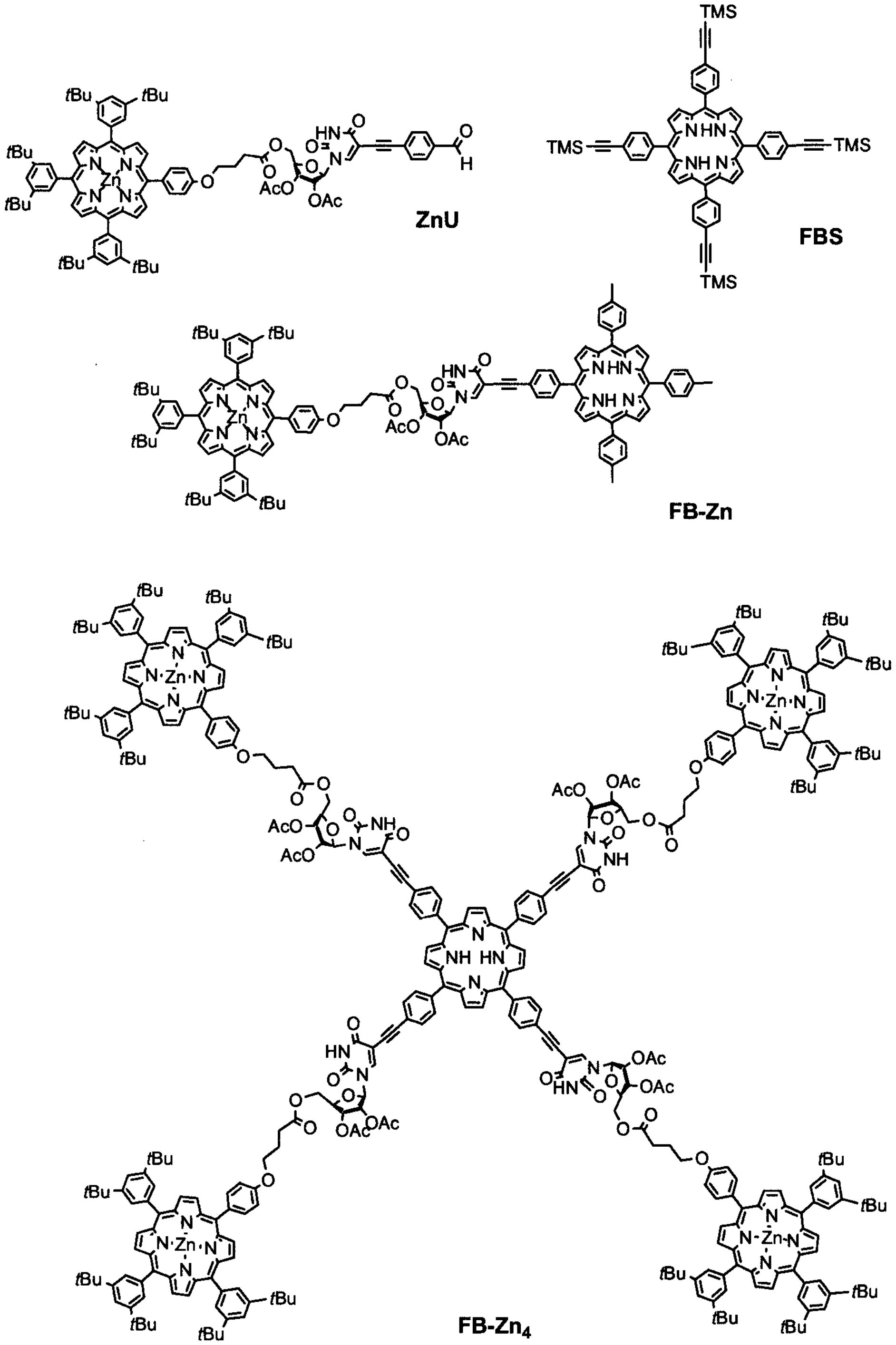

Scheme 1. The structures of the component models **ZnU** and **FBS**, the dyad **FB-Zn** and the pentad **FB-Zn$_4$**

## Results and Discussion

### Synthesis

The dyad was synthesized according to Lindsey's procedure for the construction of sterically hindered porphyrins.[7] One equivalent of aldehyde **ZnU**[6] and three equivalents of *p*-tolualdehyde were condensed, at room temperature and under an inert atmosphere, with four equivalents of pyrrole in chloroform in the presence of a catalytic amount of $BF_3 \cdot OEt_2$. The resulting porphyrinogen was then oxidized by reflux with three equivalents of *p*-chloranil, for one and a half hours. After a tedious purification requiring many chromatographic separations over silica gel, the desired dyad was isolated in 10% yield. It was characterized by $^1H$ NMR and FAB mass spectrometry ($m/z$ = 2104.5 $[M]^+$, calcd. 2104.9). The synthesis and characterization of the pentad has been reported previously.[6]

## Photoinduced Processes

### *The Dyad*

The absorption spectrum of the dyad closely matches the superposition of its two components, as shown in Figure 1, where absorption spectra of both the component units, their sum and the absorption spectrum of the dyad are given. This indicates a very modest interaction between the components, as expected from the length and type of bridging ligand.

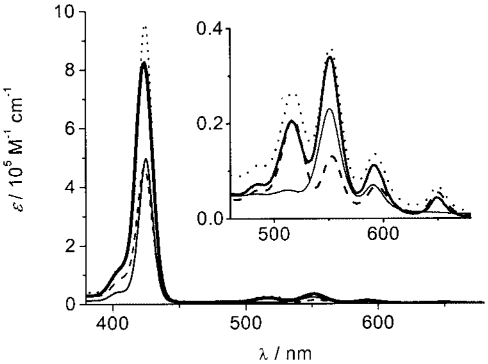

Figure 1. Molar absorption coefficients of the models **ZnU** (thin solid line) and **FBS** (dashed line), and of **FB-Zn** (thick solid line) in toluene solutions, the sum of the molar absorption coefficients of the models is also reported (dotted line)

The emission spectrum of the dyad, after excitation at a wavelength where only **FBS** absorbs, i.e. at $\lambda > 625$ nm, displays the emission spectrum of the **FBS** model, with an identical quantum yield within experimental error (Table 1). Selective excitation of the **ZnU** unit is not possible (see Figure 1) but excitation where both components absorb, yields an emission spectrum which shows the features of both the free base component ($\lambda_{max.}$= 652 and 718 nm) and of the zinc component ($\lambda_{max.}$= 598 nm and 646 nm). However, if the emission is compared to those of the component models absorbing the same number of photons as in the dyad (Figure 2), it is clear that, in the array, the emission of the zinc porphyrin unit is quenched whereas the emission of the free-base porphyrin moiety is increased, i.e. it is sensitized (Table 1).

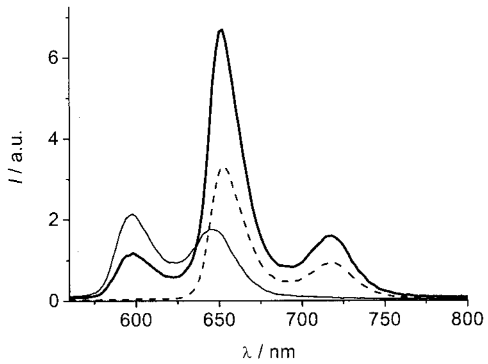

Figure 2. Emission spectra in toluene at 298 K of the models **ZnU** (thin solid line; $A_{550nm}$ = 21.6%),**FBS** (dashed line; $A_{550nm}$ = 11.7%), and the dyad **FB-Zn** (thick solid line; $A_{550nm}$ = 33.4%, the partition of photons is $A_{\mathbf{PZnU}}$ = 21.6% and $A_{\mathbf{FBS}}$ = 11.7%) in toluene solutions; excitation at 550 nm

Time-resolved experiments with picosecond resolution (at $\lambda$ = 600 nm, the maximum of the zinc porphyrin component emission) revealed a bi-exponential decay of the luminescence of the dyad, with lifetimes of 240 ps and 1.9 ns, accounting for ca. 30% and 70% of the total decay, respectively (Figure 3). Whilst the short lifetime could be due to the quenching of the luminescence of the zinc porphyrin component, the long lifetime is typical of the unquenched **ZnU** model (Table 1). The luminescence of the dyad at $\lambda$ = 720 nm (Figure 3), where only the free base component emits, is characterized by a species with a lifetime of ca 240 ps, closely matching the fast decay of the zinc porphyrin component. A subsequent slower decay of 9.8 ns, typical of the emission of the model **FBS** (Table 1), was detected on a

Table 1. Luminescence properties and energy levels of the excited states of the models and arrays in toluene

| | | 298 K | | | | 77 K | |
|---|---|---|---|---|---|---|---|
| | State | $\lambda_{max.}$ (nm) | $\varphi_{fl}$ [a] | $\varphi_{fl}$ [b] | $\tau$ (ns)[c] (% component) | $\lambda_{max.}$ (nm) | $E$ (eV)[d] |
| **FBS** | $^1$FBS | 652 | 0.18 | 0.18 | 9.5 | 646 | 1.92 |
| **ZnU** | $^1$ZnU | 598 | | 0.073 | 1.9 | 604 | 2.05 |
| **FB-Zn** | $^1$FB-Zn | 652 | 0.19 | 0.33 | 0.240[e]; 9.8 | 647 | 1.92 |
| | FB-$^1$Zn | 598 | | 0.042 | 0.240; 1.9<br>(30%); (70%) | 604 | 2.05 |
| **FB-Zn$_4$** | $^1$FB-Zn$_4$ | 652 | 0.13 | –[f] | 9.8 | 648 | 1.91 |
| | FB-$^1$Zn$_4$ | 600 | | –[f] | 0.110; 0.240; 1.9<br>(50%); (15%); (35%) | 606 | 2.05 |

[a] Emission quantum yield. Selective excitation of the free-base porphyrin unit was at 650 nm. [b] Emission quantum yield. Excitation of both free-base and zinc porphyrin components was at 550 nm. The calculation is based on the photons absorbed directly by the moiety, as calculated by the molar absorption coefficients of the models **ZnU** and **FBS**. [c] Excitation was at 532 nm or at 337 nm for lifetimes > 2 ns. [d] Energy levels from the emission maxima at 77 K. [e] Lifetime of the rise. [f] In this array the interaction between components is strong (see text) and this prevents a reliable calculation of the partitions of photons between components. Consequently, it was impossible to measure the emission yields as done for the dyad (see above).

longer time scale with a nanosecond time correlated single photon counting apparatus.

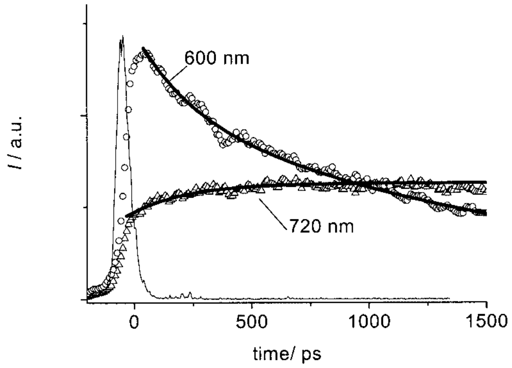

Figure 3. Time-resolved luminescence of **FB-Zn** in toluene solution after excitation at 532 nm; decay at 600 nm (open circles) and 720 nm (open triangles) with the bi-exponential fitting with lifetimes of 240 ps and 1.9 ns at 600 nm and of 240 ps and 9.8 ns at 720 nm; the exciting flash profile is also shown

The energy of the emission maxima, determined at 77 K, are conventionally assumed to correspond to the energy levels of the emitting states. From these, a value of 2.05 eV and 1.91 eV was derived for the energy of the singlet excited states localized on the zinc porphyrin and the free-base unit, respectively. The energy transfer from the zinc to the free-base porphyrin component is thermodynamically allowed and has a driving force of 0.14 eV. Therefore, the quenching of the zinc porphyrin donor and the sensitization of the free-base porphyrin acceptor are interpreted as being due to an energy transfer process. The rate constant can be calculated from the equation $k = 1/\tau - 1/\tau_0$, where $\tau$ and $\tau_0$ are the lifetime of the quenched component (240 ps) and of the model compound (1.9 ns), respectively. The resulting rate constant is $k = 3.6 \times 10^9$ s$^{-1}$. However, the bi-exponential nature of the decay indicates that only a fraction (30%) of the donor is quenched, whereas the main part (70%) is largely unaffected with respect to the model lifetime. This is indicative of the existence of two different conformers of the dyad (see below).

The occurrence of energy transfer from the zinc porphyrin unit to the free-base porphyrin unit is further supported by the excitation spectrum detected at 720 nm, where only the free-base porphyrin emits, which shows the contribution from the **ZnU** band at 550 nm, indicating that the emission of the free-base is sensitized by the absorption of the zinc component (Figure 4). The overlap between absorption spectrum and excitation spectrum of the dyad is not complete since the sensitization of free-base porphyrin by the zinc component only takes place in 30% of the excited conformation.

Energy transfer between singlet states can occur by two different mechanisms: the Förster mechanism (or dipole−dipole interaction)[8] or the Dexter mechanism (or electron exchange).[9] In case of energy transfer between singlet states with high absorbances and high emission quantum yields, the dipole−dipole mechanism usually prevails. For this mechanism, it is possible to calculate the rate $k_{\mathrm{en}}^{\mathrm{F}}$ by means of Equation (1),[8] in which $\Phi$ and $\tau$ are the emission quantum yield (0.073) and lifetime (1.9 ns) of the donor **ZnU**, respectively, $d_{\mathrm{DA}}$ is the donor−acceptor center-to-center distance, $n$ is the refractive index of toluene and $J^{\mathrm{F}}$ is the overlap integral. $\kappa^2$, the orientation factor, takes into account the relative orientation of the transition dipole moments of the donor and the acceptor and in a pair of reactants freely diffusing in solution the value is statistical, i.e. 2/3, since they can randomly approach. In the present case, the statistical value 2/3 can be considered a good approximation because of the length and flexibility of the bond connecting the two components.

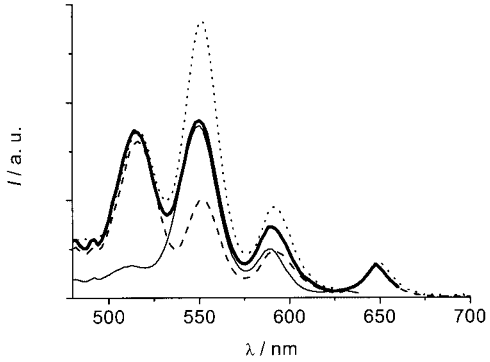

Figure 4. Excitation spectrum registered at $\lambda_{\mathrm{em}} = 720$ nm (thick solid line) and an arbitrarily scaled absorption spectrum (dotted line) of **FB-Zn** in toluene solution; for comparative, purposes the excitation spectra of models **ZnU** at $\lambda_{\mathrm{em}} = 646$ nm (thin solid line) and **FBS** at $\lambda_{\mathrm{em}} = 720$ nm (dashed line) are also shown

$$k_{en}^{F} = \frac{8.8\times10^{-25}\kappa^{2}\Phi}{n^{4}\tau d_{DA}^{6}}J^{F} \qquad (1)$$

The Förster overlap integral, $J^{\mathrm{F}}$, is calculated from the overlap between the luminescence spectrum of the donor **ZnU**, $F(\bar{\nu})$ (cm$^{-1}$ units) and the absorption spectrum $\varepsilon(\bar{\nu})$ of the acceptor **FBS** (cm$^{-1}$ units), according to Equation (2).[8]

$$J^{F} = \frac{\int F(\bar{\upsilon})\varepsilon(\bar{\upsilon})/\bar{\upsilon}^{4}d\bar{\upsilon}}{\int F(\bar{\upsilon})d\bar{\upsilon}} \qquad (2)$$

From the experimental emission and absorption spectra, an overlap integral $J^{\mathrm{F}}$ of $5.55 \times 10^{-14}$ cm$^3$ M$^{-1}$ was calculated, and from Equation (1) a critical transfer distance $R_{\mathrm{c}}$ of 28 Å was calculated. This is the distance at which the energy transfer rate equals the intrinsic deactivation rate of the donor and, given the sixth power dependence [see Equation (1)], for distances slightly larger, no energy transfer can occur because the intrinsic deactivation prevails. From Equation (1), the distance $d_{\mathrm{DA}}$, at which the transfer occurs with the experimental rate of $3.6 \times 10^9$ s$^{-1}$, can be calculated as being ca. 20 Å.

The presence of two different lifetimes in the decay of luminescence of the zinc donor component can be assigned to the presence of two different conformations of the dyad.

In order to elucidate this point, a series of calculations based on the semiempirical AM1 hamiltonian[10] were carried out to describe a minimum conformation for this compound in vacuo. It was found that the most stable conformation corresponds to a bent structure, with a torsion angle of 67° defined by the C2′−C1′−N1−C6 atoms, and a heat of formation of 1174 kcal/mol. The C1′ and C2′ atoms are in the ribose unit and the N1 and C6 (C6 is the carbon atom involved in the double bond) are in the uracil nucleic base. In this conformation, the distance between the two chromophores Zn and FB is 23 Å, i.e. a distance in reasonable agreement with that calculated from the experimental energy transfer rate according to the Förster theory (ca. 20 Å, see above). However, we note that the molecule is quite free to rotate about the saturated bridges and that small variations of the torsion angle mentioned above lead to negligible variations in the overall energy of the compound. For example, a small increase in the twisting angle mentioned above, from 67° to 97°, leads to distances d−d greater than 28 Å, but the corresponding destabilization of the molecule is only 0.5 kcal/mol. It is quite possible that interaction of this molecule with a suitable solvent stabilizes an energy minimum corresponding to a donor−acceptor distance of at least 30 Å. Such a distance implies a reduced and, possibly, a no more competitive rate constant for the energy transfer process. The greatest distance achieved by rotation around the above twisting angle is ca. 32 Å.

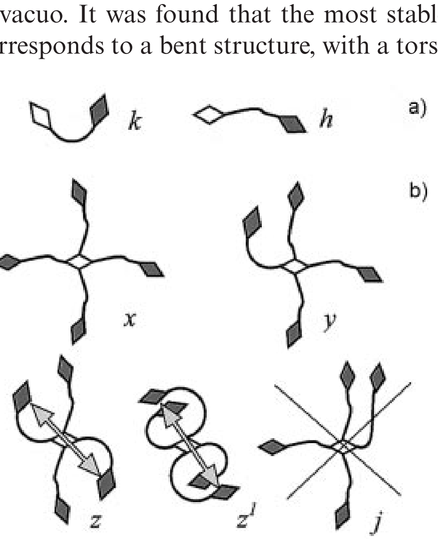

Scheme 2. Cartoon representation of the different conformations for **FB-Zn** (a) and **FB-Zn$_4$** (b); white diamonds represent the free-base porphyrin energy acceptor and gray diamonds the Zn porphyrin energy donor; the arrows indicate exciton interactions

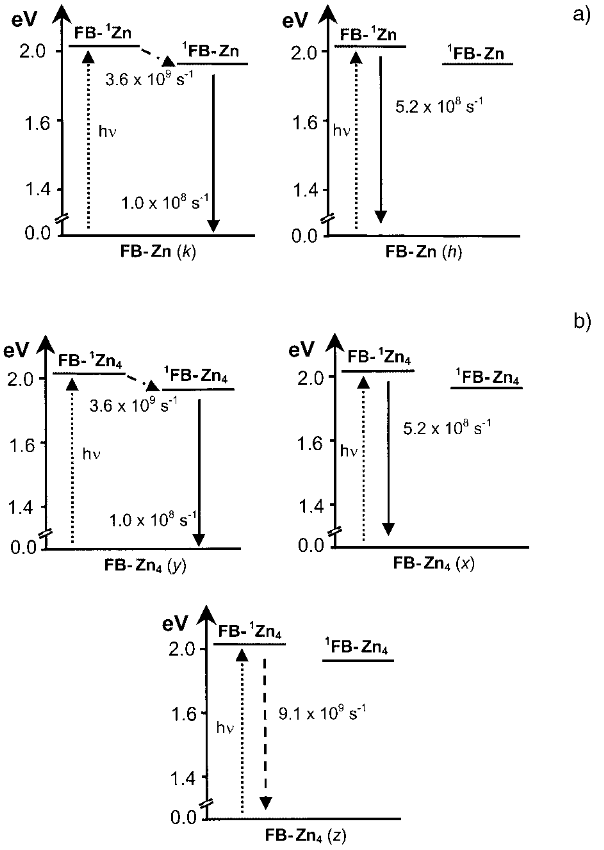

Scheme 3. Energy level scheme and photoinduced processes which can occur in the different conformations of **FB-Zn** (a) and **FB-Zn$_4$** (b); dotted lines represent light absorption, dashed lines represent non-radiative transitions, solid lines are radiative processes and dash-dot lines, energy transfer

On this basis, we interpret the results of the photoinduced processes in the dyad **FB-Zn** as follows. The dyad is composed of two populations of conformers which equilibrate on a long time scale compared to the photoinduced processes and therefore behave as independent species. Although the theoretical results in the gas phase indicate a folded structure as a shallow minimum conformer, the solution experimental results indicate that a more displaced conformation has been stabilized by solvent interactions and accounts for 70% of the population. A schematic illustration of the two conformers, whose structures are compatible with both the experimental findings and the theoretical results, is shown in Scheme 2 (a). Both conformers are in a bent configuration. However, in isomer *k* (Scheme 2, a) the two porphyrins are nearly overlapping, with a distance of the order of 20−23 Å between the donor−acceptor couple, which is sufficient to promote a dipole−dipole type energy transfer process. In the second open conformation, *h*, the planes containing the porphyrins are displaced and the center-to-center distance is increased to a value of ca. 32 Å, which does not allow Förster energy transfer to take place effectively.

Scheme 3 (a) shows schematic energy level diagrams illustrating the photoinduced processes occurring in both conformations of **FB-Zn**.

### *The Pentad*

Unlike that found for the dyad, the absorption spectrum of the pentad **FB-Zn$_4$**, does not result from the simple superposition of the spectra of the component units. Figure 5 shows the absorption spectrum of the pentad compared with the sum of its components. Large effects on the Soret band, namely broadening, decrease in epsilon and a minor red shift are observed and, in addition, a rather important change in epsilon, a red shift and a change in spectral shape in the Q band region are also observed. Whenever porphyrins are connected to other species, some change in the Soret band region, which corresponds to the $S_0-S_2$ transition, is generally encountered. However, the effect on the Q band region, which corresponds to the $S_0-S_1$ transition, is rather unusual. This observation can be taken as indication of a rather important coupling between components. Since the type and length of the linker is not expected to couple the components substantially, a through-space interaction can be invoked to explain this observation. This must occur in a conformation where the components are in close contact and which can only be possible in **FB-Zn$_4$** and not in **FB-Zn**, since no such interaction was apparent in the latter.

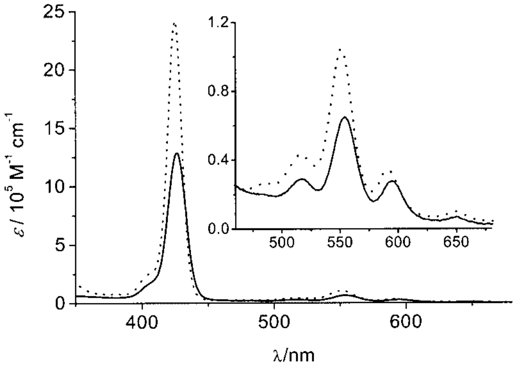

Figure 5. Molar absorption coefficient of **FB-Zn$_4$** in toluene solution (solid line); the sum of the molar absorption coefficients of the components, one **FBS** and four **ZnU** units, is also reported (dotted line)

Selective excitation of the free-base component at 650 nm results in a decrease of the emission quantum yield of this component compared to its model, from 0.18 to 0.13 (Table 1). This confirms the perturbation of the radiative and non-radiative parameters of the units when they are incorporated into the pentameric array. Under these strong coupling conditions, a quantitative consideration of the emission quantum yields of the individual components of the pentad as performed in Figure 2 for the dyad, is rather unreliable. In fact, that type of determination relies strongly on the fact that the properties of the components are not substantially modified when incorporated into the arrays. It is evident from both the ground state absorption spectrum (Figure 5) and from the free-base porphyrin emission yield (Table 1), which appears decreased in the pentad, that this is not the case. A qualitative experiment comparing the overall emission quantum yield of optically matched solutions of the dyad and the pentad is presented in Figure 6. This shows that the emission in the higher order array is strongly diminished for both the zinc porphyrin and the free-baseporphyrin. This cannot be attributed to an increased efficiency of the intramolecular energy transfer process, but rather to an overall increase in the non-radiative decay involving both components of the pentad, i.e. the free-base porphyrin and the Zn porphyrin.

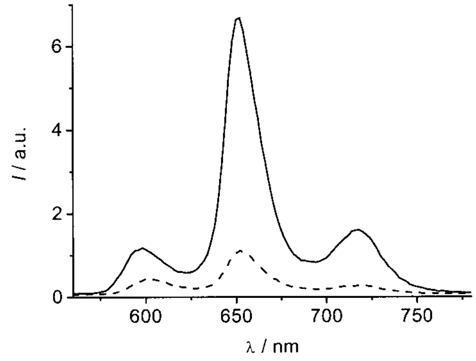

Figure 6. Emission detected from optically matched ($A$ = 0.18) toluene solutions of **FB-Zn** (solid line) and **FB-Zn$_4$** (dashed line) after excitation at 550 nm

Upon excitation at 532 nm, the time-resolved luminescence of the pentad **FB-Zn$_4$** is reduced with respect to that of an optically matched **FB-Zn** dyad. The initial intensity at 600 nm is ca. 25% that of the dyad. A satisfactory fit of the decay at 600 nm, illustrated in Figure 7, was obtained using three exponentials of 110 ps (50%), 240 ps (15%) and 1.9 ns (35%). In this case, the band at 720 nm typical of the free-base porphyrin emission, is extremely low because of the numerical predominance of the zinc porphyrin chromophore, and no rise in the luminescence signal could be detected.

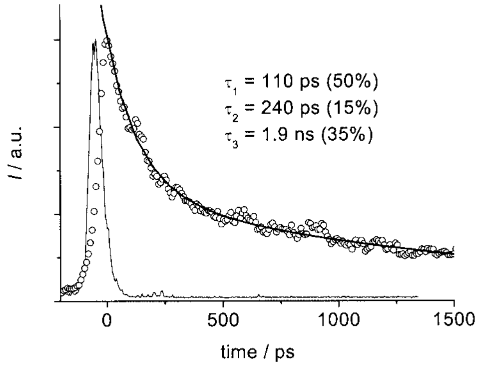

Figure 7. Time-resolved luminescence of **FB-Zn$_4$** in toluene solution after excitation at 532 nm; decay at 600 nm (O) and tri-exponential fitting with lifetimes of 110 ps, 240 ps and 1.9 ns. The exciting flash profile is also shown

The two longest lifetimes, 1.9 ns and 240 ps, are similar to those found in the dyad **FB-Zn**, and can be similarly assigned to unquenched conformations (1.9 ns), where the donor and acceptor are at the extremities of an extended linker and to quenched conformations (240 ps) with the donor and the acceptor at the extremities of a bent linker. The shortest (110 ps) and most important component in the luminescence decay, which accounts for ca. 50% of the intensity, is new and may be assigned to a different type of conformer which is only possible in the pentad. Multi-exponential decay of the zinc porphyrin luminescence is typical of flexible zinc porphyrin-based star compounds with a central free base porphyrin energy acceptor and has been frequently reported in the literature.[4k−4l]

In spite of the fact that the overall yield of the luminescence of the pentad is extremely low, sensitization of the free-base by the zinc component still occurs, as illustrated by the excitation spectrum registered at 720 nm, which is a wavelength normally indicative of free-base porphyrin emission (Figure 8). In this excitation spectrum, there is a clear contribution to the free-base emission from the zinc porphyrin donor band at 550 nm. Its extent is partial as in the dyad **FB-Zn**, and may be assigned to the fact that some conformations in **Fb-Zn$_4$** do not contribute to energy transfer. In spite of the fact that we could observe some sensitization of the free-base emission by the zinc porphyrin component (see Figure 8), the overall emission of the free-base porphyrin does not appear to increase in the pentad but rather to decrease, as shown in Figure 6. At the same time, we determined a quenching of the zinc porphyrin luminescence without detecting a corresponding sensitization in the free-base acceptor. A similar behavior was reported by Sanders et al. for a pentaporphyrin composed of a free base tetrapyridylporphyrin core coordinated via four axial bonds to a cyclic tetra-Zn porphyrin.[4s] The authors assigned the quenching of the luminescence of both components to an undefined photoinduced electron transfer process. In the present case, no photoinduced electron transfer can occur spontaneously since, according to their redox potentials,[6] the energy of the highest excited state (2.05 eV, Table 1) is insufficient to promote an electron transfer between the components. Therefore, in order to explain this observation, we have to assume that a remarkable loss of emission from the zinc porphyrin component, as well as from the free-base porphyrin unit, must take place through some non-radiative path.

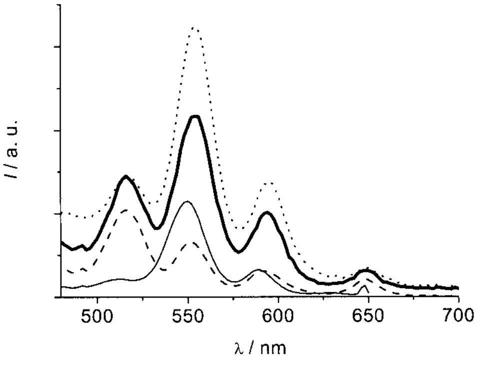

Figure 8. Excitation spectrum registered at $\lambda_{em}$ = 720 nm (thick line) and absorption spectrum (dotted line) of **FB-Zn$_4$** in toluene solution; for comparative, purposes the excitation spectra of the models **ZnU** at $\lambda_{em}$ = 646 nm (thin solid line) and **FBS** at $\lambda_{em}$ = 720 nm (dashed line) are shown; the spectra are arbitrarily scaled

Some strong interacting conformer could account for the observed phenomena, namely non-additivity of absorption and a dramatic decrease in emission quantum yield of the pentad compared to the dyad as well as a new fast component (110 ps) in the quenching of the luminescence. This conformation must be precluded in the dyad, where the above effects were not observed. For the pentad, a series of different conformations can be envisaged, some of which are shown in Scheme 2 (b.) Conformation *x* (fully extended) and conformation *y* (partially bent) resemble the respective conformations of the dyad and should behave similarly. However, the conformations resulting from the concomitant bending of two (or more) Zn porphyrins over the free base component, denoted as *z* or $z^1$, are unique to the pentad. Other types of conformations unique to the pentad, denoted as *j*, with the Zn porphyrins in a parallel arrangement, can be neglected. In fact, it seems unlikely that this type of conformation could affect the radiative parameters of the free-base component which is not involved in the interaction. Therefore, type *z* conformers are most likely responsible for the strong interaction observed in the pentad and this is supported by the data presented in the following sections.

A simplified interpretation of the data can be attempted as follows. The pentad is assumed to take (at least) three different types of conformations denoted as *x*, *y* and *z*. Conformations *x* and *y* behave “regularly” i.e. similarly to the corresponding bent or extended conformations in the dyad, as confirmed by the similar lifetimes detected in the luminescence quenching of the Zn porphyrin donor. The *z* type conformations may be responsible for the different behavior of the pentad array compared to the dyad. The short luminescence lifetime of the zinc porphyrin component (110 ps) is assigned to this type of conformation which, unlike the 240 ps component assigned to an energy transfer process in conformation *y*, has to be regarded as a fast, non-radiative decay of the excited state. In this type of conformation, an electronic, exciton type interaction also involving the free-base component, can occur. This induces a strong perturbation of the individual parameters of the components resulting in a greatly increased non-radiative decay. Since it accounts for about half of the excited state population, as calculated from the luminescence of the components, its behavior dominates the observed phenomena.

The ensemble Zn−FB−Zn in *z*, or Zn−Zn−FB−Zn−Zn in $z^1$, typical of the pentad, is therefore deemed responsible for the new properties, caused by the strong electronic coupling between the components. Deactivation of the excited ensemble Zn−FB−Zn (or Zn−Zn−FB−Zn−Zn) proceeds rapidly, by non-radiative pathways, without producing any sensitization localized at the free-base. The free-base itself, when selectively excited, displays a decreased emission quantum yield in the pentad. This indicates that, irrespective of the excited component, the Zn−FB−Zn ensemble seems to follow non-radiative decay paths.

Further evidence supporting the importance of a conformation where the free-base porphyrin is somehow shielded from the exterior is given by the electrochemistry[6] and the triplet excited state lifetime data reported below.

A nanosecond flash photolysis experiment on the pentad **FB-Zn$_4$** in air free solution allows detection of the porphyrin triplet states of the zinc porphyrin donor and of the free-base porphyrin acceptor. The lifetime of the triplet state localized on the zinc porphyrin, FB-$^3$Zn$_4$, decays with a lifetime of 0.5 μs and sensitizes the lower energy triplet localized on the free-base porphyrin $^3$FB-Zn$_4$, which has a lifetime of 500 μs, much higher than that measured in the model **FBS** and in the dyad **FB-Zn** which are, under the same conditions, 200 μs and 160 μs, respectively (Figure 9). This indicates that the reactive FB-$^3$Zn$_4$ excited state of the pentad is better shielded from trace impurities and oxygen contained in the solvent than in the models and the dyad, and supports the assignment of a rather compact structure which protects the central free-base porphyrin, as in the *z* conformations.

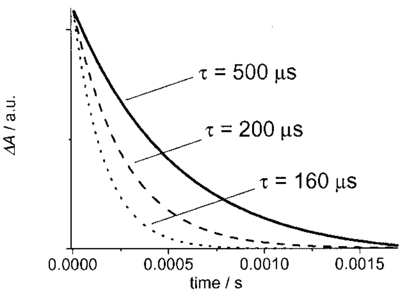

Figure 9. Normalized decay for absorption of the free-base triplet excited state in the model, $^3$FBS (dashed line), in the dyad, $^3$FB-Zn (dotted line), and in the pentad, $^3$FB-Zn$_4$ (full line)

A similar indication comes from electrochemistry, which was reported previously.[6] The central free-base porphyrin behaves as an encapsulated electroactive molecule in pentaporphyrin **FB-Zn$_4$**, which is masked from electron transfer by the experimental conditions employed. The electrochemical studies make it clear that, in a flexible molecule such as pentaporphyrin **FB-Zn$_4$**, a substantial reduction of the electron transfer rate to the porphyrin core may be reasonably expected, i.e. the restricted accessibility to this core is probably assignable to conformational effects rather than to steric factors alone.

Scheme 3 shows the type of photoinduced processes which can occur in the arrays for extended (*x*), singly bent (*y*) or multiply bent (*z*) conformations.

### Circular Dichroism Spectroscopy

In order to obtain further insight into the type and strength of interactions postulated in the different conformational cases, circular dichroism experiments were performed. The models **FBS** and **ZnU** display no optical activity when excited at the absorption bands of the porphyrin, while both **FB-Zn** and **FB-Zn$_4$** are optically active. Data from CD experiments for the dyad and the pentad in the Soret band region are shown in the upper panel of Figure 10 while the lower panel shows the electronic absorption bands for comparative purposes.

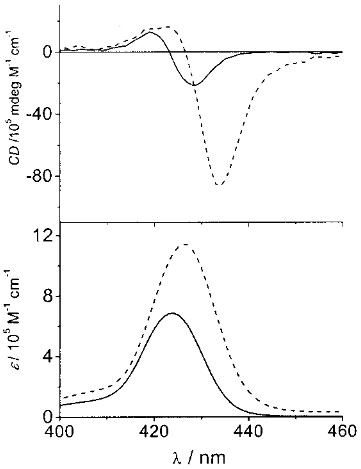

Figure 10. CD (upper panel) and UV (lower panel) spectra of **FB-Zn** (solid line) and **FB-Zn$_4$** (dashed line) in toluene solutions

The zero value of the CD signal at the wavelength of the maximum UV/Vis absorption band, together with the lack of signal for the separate units composing the pentad, indicates exciton coupling as the origin for the observed CD spectrum. In the simple case of the dyad, the CD spectrum arising from the exciton coupling between Zn and FB was calculated and the results obtained for the Soret band region are displayed in Figure 11. The molecular geometry used in the calculations was that obtained from the AM1 optimization, corresponding to the conformation *k* in Scheme 2 (a). The protocol described by Tinoco [11] for exciton coupling in the case of strongly allowed transitions was implemented by using energies and transition dipole moments calculated with the ZINDO/S program.[10]

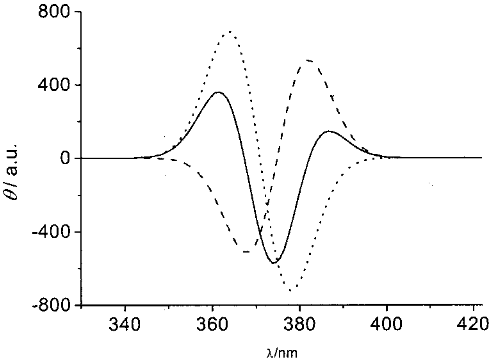

Figure 11. Calculated CD spectrum for the dyad **FB-Zn**; the solid line results from the sum of the exciton splitting of the parallel (dotted line) and perpendicular (dashed line) components of the Soret band

The calculations show that the crossed interactions between the two Soret states of **ZnU** and **FBS** give rise to two exciton bands of opposite sign (represented by the dotted and dashed curves in Figure 11), with a resulting component (solid line) presenting a dissymmetric pattern, the negative part being larger and at longer wavelength than the positive one. The other, smaller component calculated on the low energy side was not detected experimentally, and is derived from a direct inclusion of the two transition dipole components typical of the Soret band. In fact, usually just the parallel component of the band is included in the calculation, as the perpendicular one is partially deleted by the librational modes, as recently shown for similar compounds.[12] While the calculated energy appears, as usual, shifted to the blue when using the ZINDO/S program, the pattern and intensity of the signals appear consistent with experiment and, since the calculated CD spectrum appears very sensitive to the geometry adopted, these results corroborate the conformational hypotheses presented above.

## Complexation

Zinc porphyrins are known to axially bind pyridine or pyridyl residues with association constants of the order of $10^4$ M$^{-1}$. These constants have been found to increase dramatically up to ca. $10^8$ M$^{-1}$ when multiple bonds contribute to the complex formation (cooperative effect).

We have undertaken these experiments with both monodentate and bidentate pyridyl complexing agents in order to obtain information about the geometry of and the interactions between the zinc porphyrin chromophores. We have derived the association constants using different methods and additionally, we have monitored the effect of full complexation on several spectroscopic properties (i.e. luminescence and CD spectroscopy) with the aim of further understanding these systems.

Association of a pyridyl residue to Zn porphyrin induces a red shift, both on the Soret and Q absorption bands, and on the emission spectrum of the zinc porphyrins. A typical example is shown in Figure 12 for complexation of **ZnU** by pyridine (PYR). The spectral change, which is proportional to the concentration of complex, can be treated according to the equation below, which has been adapted and developed previously.[4j,13]

$$Obs = Obs_0 + \frac{\Delta Obs}{2S_0}\left\{K_d + X + S_0 - \left[(K_d + X + S_0)^2 - 4XS_0\right]^{1/2}\right\} \tag{3}$$

In this equation, the association constant $K_{\text{ass}}$ is $1/K_d$, *Obs* is any observed signal intensity (i.e. absorbance or emission intensity), $S_0$ is the concentration of **ZnU**, or **FB-Zn** or **FB-Zn$_4$** (constant), $X$ is the concentration of the complexing agent (variable), $\Delta Obs$ is the maximum variation of the observed signal intensity under examination. The fitting of the absorbance data points of the maximum of the Soret band absorbance of the complexed form, at 431 nm, and the fitting of the emission intensity at λ = 610 nm are given in the insets of Figure 12.

Binding of the bidentate 1,4-diazabicyclo[2.2.2.]octane, DABCO, to Zn porphyrins to form a 1:2 complex has been reported to induce a shift in the UV-absorbance of the 1:1 complex by ca. 6 nm, caused by exciton coupling between the parallel porphyrin units.[14] Therefore, titration of the pentad with DABCO could give an indication of a simultaneous complexation of two porphyrins.[15] As illustrated in Figure 13, the complexation behavior of **FB-Zn$_4$** by DABCO is similar to that of **ZnU** by PYR. A single isosbestic point can be observed, indicating that only the uncomplexed and the 1:1 complex are present without any intermediate 2:1 (Zn porphyrin/DABCO) complex formation. This is indicative of the fact that in **FB-Zn$_4$** there are no couples of Zn porphyrins available for a cooperative binding. Further support for this observation comes from the comparison of the association constants derived by absorp-

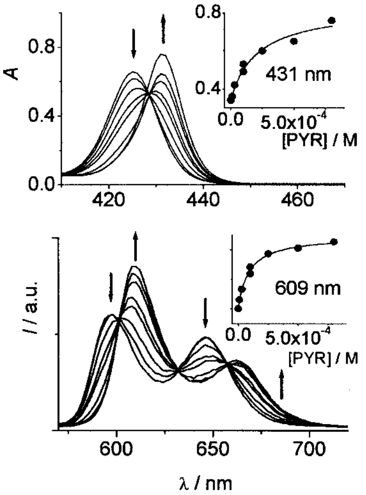

Figure 12. Electronic spectra of **ZnU** in toluene solution upon titration with increasing amounts of PYR; the upper panel shows the change of absorbance in the Soret band region and the inset shows the data points at 431 nm fitted according to Equation (3); in the lower panel, the change in emission intensity is shown and the inset shows the data points at 609 nm fitted according to Equation (3)

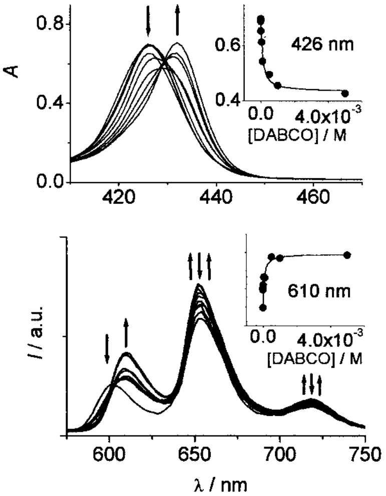

Figure 13. Electronic spectra of **FB-Zn$_4$** in toluene solution upon titration with increasing amounts of DABCO; change of absorbance in the Soret band region appears in the upper panel with the fitting of the data points at 426 nm according to Equation (3) shown in the inset; change in the emission intensity is reported in the lower panel with the fitting to data points at 610 nm according to Equation (3) shown in the inset

Table 2. Association constants in toluene

| | PYR | | DABCO | | BIPY | |
|---|---|---|---|---|---|---|
| | Abs[a] $K_{ass}$ (M$^{-1}$) | Em[b] $K_{ass}$ (M$^{-1}$) | Abs[a] $K_{ass}$ (M$^{-1}$) | Em[b] $K_{ass}$ (M$^{-1}$) | Abs[a] $K_{ass}$ (M$^{-1}$) | Em[b] $K_{ass}$ (M$^{-1}$) |
| **ZnU** | $8 \times 10^3$ | $9 \times 10^3$ | $2 \times 10^5$ | $4 \times 10^5$ | $2 \times 10^4$ | $2 \times 10^4$ |
| **FB-Zn** | $5 \times 10^4$ | $9 \times 10^4$ | $5 \times 10^4$ | $5 \times 10^4$ | $2 \times 10^4$ | $5 \times 10^4$ |
| **FB-Zn$_4$** | $2 \times 10^4$ | $3 \times 10^4$ | $1 \times 10^4$ | $1 \times 10^4$ | $5 \times 10^4$ | $2 \times 10^4$ |

[a] Determined by spectrophotometric titration. The absorbance signal at $\lambda = 431 \pm 1$ was fitted to the equation given in the text. [b] Determined by spectrofluorimetric titrations upon excitation at the isosbestic of the absorption bands of uncomplexed and complexed forms, $\lambda = 428 \pm 1$. The emission signal at $\lambda = 610$ nm was fitted to the equation given in the text.

tion and emission methods. Table 2 shows these association constants determined for **ZnU**, **FB-Zn** and **FB-Zn$_4$** with PYR, DABCO and 4,4′ bipyridine (BIPY), respectively. The association constants of bidentate DABCO and BIPY with the dyad and pentad do not appear to differ substantially from the model **ZnU**. This indicates that the multiple binding sites of the pentad, compared to the model **ZnU** and the dyad **FB-Zn** are not detected by the bidentate complexing agent and confirms that the Zn porphyrin units in the pentad are not available for a cooperative binding, either because they are engaged in some different type of interaction, or because they cannot approach each other at an appropriate distance to complex at both ends of the bidentate units.

As a further experiment to help in the interpretation of the data, we observed the kind of changes in the emission and CD spectra brought about by complexation of the dyad and pentad with mono or bidentate bases. Figure 14 shows examples of the changes in the emission spectra occurring upon complexation of BIPY (concentration of complex > 95%) with the model **ZnU**, the dyad **FB-Zn** and the pentad **FB-Zn$_4$**. The results obtained using PYR and DABCO in place of BIPY (not reported) are essentially the same. In the axially bound model **ZnU**, maxima at 609 nm and 662 nm, compared to 598 nm and 646 nm in unbound **ZnU**, appear and an increased intensity of the first band (ratio 1.36) and a decrease in the intensity of the second band (ratio 0.7) with respect to unbound **ZnU** can be seen. Comparison of the emission spectra in Figure 14 confirms that the changes in the emission spectra of the dyad and the pentad can be ascribed only to the different luminescent properties of the axially coordinated zinc porphyrin. No other effect due to changes in the emission properties of the zinc porphyrin in the arrays can be detected.

An experiment similar to the one described for the emission experiment, was also carried out for the CD spectra. CD spectra of the dyad **FB-Zn** (middle panel) and the pentad **FB-Zn$_4$** (bottom panel) before and after complexation with BIPY (complex concentration > 95%), respectively, are shown in Figure 15. The spectrum for **ZnU**, where no signal was detected since it is not optically active, is given in the top panel for purposes of comparison. In **FB-Zn**, the CD signal was slightly shifted, similarly to the shift occurring in the absorption spectrum of the complexed **FB-Zn** as expected for an exciton coupling interaction. This indicates

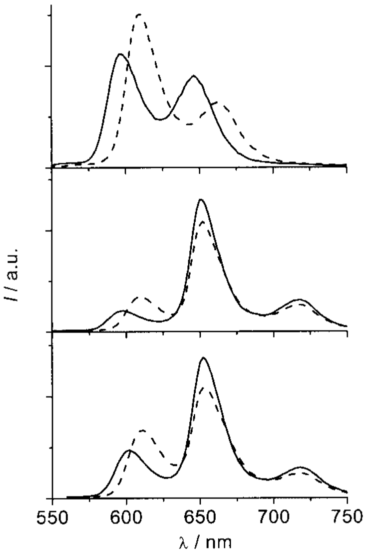

Figure 14. Emission spectra of **ZnU** (top panel), **FB-Zn** (middle panel) and **FB-Zn$_4$** (lower panel) in toluene solutions before (solid line) and after (dashed line) addition of BIPY (concentration of the complex > 95%)

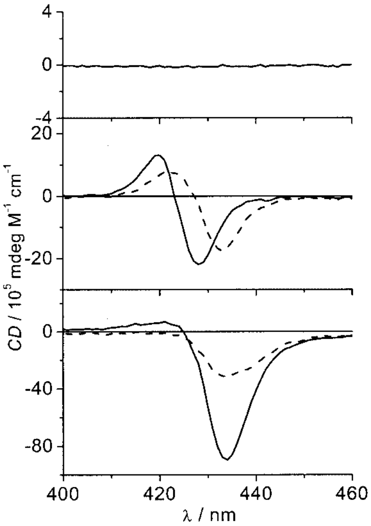

Figure 15. CD spectra of **FB-Zn** (middle panel) and **FB-Zn$_4$** (lower panel) in toluene solutions before (solid line) and after (dashed line) addition of BIPY (concentration of the complex > 95%); the top panel shows the signal obtained for the model **ZnU** for comparative purposes

that the presence of BIPY does not alter the type of interaction in conformer *k*, which is responsible for the CD signal, as discussed in the previous section. Conversely, in the pentad **FB-Zn$_4$** axial binding to the zinc porphyrin unit by BIPY has a stronger effect on the signal. There was no shift, but a sizeable decrease of the CD band intensity was observed. The results obtained using DABCO or PYR are essentially the same.

An attempted interpretation of the results presented above follows. An increase in the luminescence would be expected if the postulated non-radiative decay responsible for the decrease in the luminescence yield of the pentad and for the rapid quenching assigned to non-radiative decay (110 ps) of the zinc porphyrin luminescence, is caused by a direct interaction between two zinc porphyrins. In that case, complexation by a bidentate BIPY should disrupt such an aggregate and re-establish the luminescence. The absence of this effect on the luminescence upon BIPY binding confirms that configuration *j* in Scheme 2 cannot be responsible for the detected decrease in luminescence yield.

If the CD spectra are considered, the behavior of **FB-Zn** is quite regular − upon complexation there is no disruption of the interaction responsible for exciton coupling, just a slight shift, which is in agreement with the change in the absorption spectrum of the complex form. This probably indicates that complexation of the Zn porphyrin in conformation *k*, occurs on the Zn porphyrin face remote from the free-base unit. In the case of the pentad, the situation is less straightforward. The complexing bases are unable to suppress the optical activity but modify it substantially. Whether this is indicative of the disruption of some exciton coupling in the pentad or just of a change in the parameters (distance, angles) caused by BIPY complexation, with a consequent cancellation of exciton contributions, is difficult to say. As a consequence, the existence of a conformer with more than two zinc porphyrins in a bent conformation over the central free-base, as in $z^1$, can not be excluded. In fact, in the latter case, complexation of the more internal Zn porphyrin would require some displacement or decoupling of the external Zn-porphyrin.

## Conclusions

In conclusion, we have shown that the photoinduced processes in an **FB-Zn** dyad, covalently joined by a flexible nucleosidic linker, can be rationalized on the basis of the existence of two different conformers accounting, respectively, for ca. 30% and ca. 70% of the population. The major conformer is an extended one in which the distance between chromophores does not allow energy transfer to occur, while the minor conformer is a bent one where the shorter distance between chromophores allows energy transfer by a Förster mechanism with a rate of $3.6 \times 10^9$ s$^{-1}$. This latter bent isomer is assigned to the detected CD spectrum, which is deriving from the excitonic coupling of the electric transition dipole moments of the Soret band.

The corresponding pentad **FB-Zn$_4$** exhibits extremely complex behavior, which can only be explained by the existence of three different conformers. The two first identified conformers, which account for ca. 35% and 15% , respectively, correspond to one approximately extended conformation with a distance between chromophores which inhibits energy transfer, and one bent conformation with a distance that allows energy transfer toward the free-base porphyrin core to occur. These first two conformers are similar to those observed for the dyad **FB-Zn**. However, the most striking feature in this pentaporphyrin **FB-Zn$_4$** is the observed overall decrease in the luminescence quantum yield. This is attributed to the presence of a third conformer, which is only possible in the pentamer and accounts for ca. 50% of the population. In this conformer, a very fast, non-radiative decay of the excited state of the zinc porphyrin units (rate of ca. $10^{10}$ s$^{-1}$) is also associated with a decrease in the radiative rate constant of the central free-base porphyrin. On the basis of this evidence, a strongly interacting geometry, where Zn porphyrins are folded over the central free-base porphyrin, is assigned to this conformer. CD spectroscopy data, complexation experiments with mono and bidentate bases, electrochemistry results and reactivity of the excited states with external quenchers, all provide further support to the postulated model.

## Experimental Section

**Synthesis of the Dyad (FB-Zn):** *p*-Tolualdehyde (49 mg, 0.41 mmol, 3 equiv.), the aldehyde **ZnU** (210 mg, 0.14 mmol, 1 equiv.) and pyrrole (36 mg, 37 µL, 0.55 mmol, 4 equiv.) were dissolved in chloroform, which had been dried with molecular sieves. $BF_3 \cdot OEt_2$ (56 µL of a 3.2 M solution in chloroform) was then added. The solution turned red immediately. The reaction mixture was stirred at room temperature under argon for one and a half hours. *p*-Chloranil (100 mg, 0.41 mmol, 3 equiv.) was then added to oxidize the porphyrinogen formed during condensation and the mixture was refluxed for one and a half hours. The acidic solution was finally neutralized by addition of $NEt_3$ (25 µL) and the solvent was evaporated. The product was purified by column chromatography over silica gel ($\Phi$ = 3 cm, *h* = 23 cm, eluent: EtOAc/hexane, 50:50 to 60:40). The desired dyad **FB-Zn** was finally isolated in 10% yield (28 mg, 0.013 mmol).

**FB-Zn:** Purple glassy product. $^1$H NMR ($CDCl_3$, 300 MHz): $\delta$ = 8.99 (s, 4 H, $H_\beta$), 8.96 (d, $^3J$ = 5.1 Hz, 2 H, $H_\beta$), 8.94 (d, $^3J$ = 5.1 Hz, 2 H, $H_\beta$), 8.87 (d, $^3J$ = 5.0 Hz, 2 H, $H_\beta$), 8.84 (d, $^3J$ = 4.6 Hz, 4 H, $H_\beta$), 8.81 (d, $^3J$ = 4.8 Hz, 2 H, $H_\beta$), 8.27 (d, $^3J$ = 8.3 Hz, 2 H, $H_B$), 8.10 (d, $^3J$ = 7.9 Hz, 2 H, $H_o$), 8.09 (d, $^4J$ = 1.7 Hz, 2 H, $H_{o''}$), 8.08 (d, 2 H, $H_{B'}$, hidden), 8.06 (d, $^4J$ = 1.7 Hz, 4 H, $H_{o'}$), 8.02 (d, 4 H, $H_{o'''}$, $^3J$ = 8.0 Hz), 7.99 (d, $^3J$ = 8.0 Hz, 2 H, $H_A$), 7.78 (t, $^4J$ = 1.6 Hz, 1 H, $H_{p''}$), 7.75 (t, $^4J$ = 1.7 Hz, 2 H, $H_{p'}$), 7.55 (d, $^3J$ = 7.9 Hz, 2 H, $H_{A'}$), 7.40 (d, $^3J$ = 6.1 Hz, 4 H, $H_{m'''}$), 7.28 (d, $^3J$ = 7.8 Hz, 2 H, $H_m$), 6.07 (d, $^3J$ = 4.6 Hz, 1 H, 1′-H), 5.50 (t, $^3J$ = 5.3 Hz, 1 H, 2′-H), 5.46 (t, $^3J$ = 5.1 Hz, 1 H, 3′-H), 4.51 (m, $^3J$ = 3.3 Hz, 2 H, 5′-H), 4.43 (t, $^3J$ = 3.6 Hz, 1 H, 4′-H), 4.37 (t, $^3J$ = 5.7 Hz, 2 H, $CH_2\gamma$), 2.99 (t, $^3J$ = 6.7 Hz, 2 H, $CH_2\alpha$, ), 2.70 (s, 3 H, 7′-$CH_3$ ), 2.52 (s, 6 H, 7-$CH_3$), 2.41 (m, $^3J$ = 4.1 and 7.0 Hz, 2 H, $CH_2\beta$), 2.16 (s, 6 H, $CH_3$ 2′,3′-OAc), 1.53 (s, 36 H, *t*Bu), 1.48 (s, 18 H, *t*Bu), −2.79 (s, 2 H, NH) ppm. MS (FAB$^+$): *m*/*z* = 2104.5 [M]$^+$, calcd. 2104.9.

**Spectroscopic and Photophysical Determinations:** Toluene (spectroscopic grade, C. Erba) was used as received. Titration experiments for the determination of association constants were performed using a constant concentration of porphyrins and variable concentrations of PYR, DABCO and BIPY. Absorption spectra were recorded with a Perkin−Elmer Lambda 9 spectrophotometer. Emission spectra were measured using a Spex Fluorolog II spectrofluorimeter equipped with a Hamamatsu R928 photomultiplier and are uncorrected unless stated otherwise. Relative luminescence intensities were evaluated from the area (on an energy scale) of the luminescence spectra corrected for the photomultiplier response. Luminescence quantum yields $\varphi$ for the components were obtained with reference to a standard zinc(II) porphyrin [Zn(II){5,10,15,20-tetrakis(4-*tert*-butylphenyl)porphyrin}] in toluene with $\varphi = 0.08$.[4h] Circular dichroism spectra were obtained with a Jasco J-710 dichrograph. Experiments at 77 K were done using quartz capillary tubes immersed in liquid nitrogen contained in a home-made quartz dewar.

Fluorescence lifetimes in the nanosecond range were determined using an IBH Time Correlated Single Photon Counting apparatus with excitation at 337 nm. Luminescence lifetimes shorter than one nanosecond were determined by an apparatus based on a Nd:YAG laser (Continuum PY62−10) with a 35 ps pulse duration, at 532 nm, 1 mJ/pulse and a Streak Camera. The luminescence signals from 1000 laser shots were averaged and the time profile was measured from the streak image in a wavelength range of ca. 20 nm about the selected wavelength. The fitting of the luminescence decays were performed by standard iterative non linear programs taking into consideration the instrumental response. Further details on the equipment can be found elsewhere.[16]

Transient absorbance in the nanosecond range made use of a laser flash photolysis apparatus based on a Nd:YAG laser (JK Lasers) delivering 532 nm pulses of 18 ns. Absorbance of the solutions at the exciting wavelength was ca 0.2 and an energy of 5 mJ/pulse was used for the determination of the spectra. In order to prevent undesired second-order T−T annihilation reactions, an energy of ca. 0.5 mJ/pulse was used for the triplet lifetime determination. Experiments were conducted in home-made, 10 mm optical path cuvettes, bubbled with argon for 5 min and sealed.

Computation of the integral overlap and of the rate for the energy transfer processes according to the Förster mechanism were performed with the use of Matlab 5.2.[17] Estimated errors are 10% on lifetimes, 20% on quantum yields and 30% on association constants. Working temperature, if not otherwise specified, was 295 ± 2 K.

The Hyperchem package [10] was used for both the conformational calculations (AM1 Hamiltonian) and the excited states properties calculations (ZNDO/S) of the free-base porphyrin and zinc porphyrin units necessary to perform the exciton coupling calculations.

## Acknowledgments

Funding from the Italian CNR and Ministero dell'Istruzione, dell'Universita' e della Ricerca (FIRB, RBNE019H9 K) and financial support from the CNRS and the French Ministry of Research to N. S. (ACI Jeunes Chercheurs) are acknowledged. C. S. thanks the Région Guyane for a grant.

---

[1] [1a] V. Balzani, F. Scandola, *Supramolecular Photochemistry*, Ellis Horwood, Chichester, **1991**. [1b]M. R. Wasielewski, *Chem. Rev.* **1992**, *92*, 435−461. [1c] D. Gust, T. A. Moore, A. L. Moore, *Acc. Chem. Res.* **1993**, *26*, 198−205. [1d] H. Kurreck, M. Huber, *Angew. Chem.* **1995**, *107*, 992−946; *Angew. Chem. Int. Ed. Engl.* **1995**, *34*, 849−866. [1e] A. Harriman, J.-P. Sauvage, *Chem. Soc. Rev.* **1996**, 41−48. [1f] D. Gust, T. A. Moore, A. L. Moore, in *Electron Transfer in Chemistry* (Ed.: V. Balzani), Wiley-VCH, Weinheim, **2001**, vol. 3, part II, pp. 272−336. [1g]A. K. Burrell, D. L. Officer, P. G. Plieger, D. C. W. Reid, *Chem. Rev.* **2001**, *101*, 2751−2796.

[2] [2a] W. Kühlbrandt, D. N. Wang, Y. Fujiyoshi, *Nature* **1994**, *367*, 614−621. [2b] G. McDermott, S. M. Prince, A. A. Freer, A. M. Hawthornthwaite-Lawless, M. Z. Papiz, R. J. Cogdell, N. W. Isaacs, *Nature* **1995**, *374*, 517−521. [2c] T. Pullerits, V. Sundström, *Acc. Chem. Res.* **1996**, *29*, 381−389. [2d] J. Deisenhofer, H. Michel, *Angew. Chem.* **1989**, *101*, 872−890; *Angew. Chem. Int. Ed. Engl.* **1989**, *28*, 829−847. [2e] R. Huber, *Angew. Chem.* **1989**, *101*, 849− 870; *Angew. Chem. Int. Ed. Engl.* **1989**, *28*, 848−869.

[3] [3a] K. M. Roth, D. T. Gryko, C. Clausen, J. Li, J. S. Lindsey, W. G. Kuhr, D. F. Bocian, *J. Phys. Chem. B.* **2002**, *106*, 8639−8648. [3b] K. F. Cheng, C. M. Drain, K. Grohman, *Inorg. Chem.* **2003**, *42*, 2075−2083.

[4] [4a] G. Kodis, P. L. Lidell, L. de la Garza, P. C. Clausen, J. S. Lindsey, A. L. Moore, T. A. Moore, D. Gust, *J. Phys. Chem. A* **2002**, *106*, 2036−2048. [4b] H. Imahori, D. M. Guldi, K. Tamaki, Y. Yoshida, C. Luo, Y. Sakata, S. Fukuzumi, *J. Am. Chem. Soc.* **2001**, *123*, 6617−6628. [4c] R. A. Haycock, A. Yartsev, U. Michelsen, V. Sundström, C. A. Hunter, *Angew. Chem.* **2000**, *112*, 3762−3765; *Angew. Chem. Int. Ed.* **2000**, *39*, 3616−3619. [4d] H. S. Cho, H. Rhee, J. K. Song, C.-K. Min, M. Takase, N. Aratani, S. Cho, A. Osuka, T. Joo, D. Kim, *J. Am. Chem. Soc.* **2003**, *125*, 5849−5860. [4e] A. Nakano, A. Osuka, I. Yamazaki, T. Yamazaki, Y. Nishimura, *Angew. Chem.* **1998**, *110*, 3172−3176; *Angew. Chem. Int. Ed.* **1998**, *37*, 3023−3027. [4f] S. Hecht, T. Emrick, J. M. Fréchet, *Chem. Commun.* **2000**, 313−314. [4g] D. Holten, D. F. Bocian, J. S. Lindsey, *Acc. Chem. Res.* **2002**, *35*, 57−69. [4h] I. M. Dixon, J.-P. Collin, J-P. Sauvage, L. Flamigni, *Inorg. Chem.* **2001**, *40*, 5507−5517. [4i] L. Flamigni, M. R. Johnston, L. Giribabu, *Chem. Eur. J.* **2002**, *8*, 3938−3947. [4j] L. Flamigni, A. M. Talarico, F. Barigelletti, M. R. Johnston, *Photochem. Photobiol. Sci.* **2002**, *1*, 190−197. [4k] M-S. Choi, T. Aida, T. Yamazaki, I. Yamazaki, *Chem. Eur. J.* **2002**, *8*, 2668−2678. [4l] K. Kano, R. Nishiyabu, T. Yamazaki, I. Yamazaki, *J. Am. Chem. Soc.* **2003**, *125*, 10625−10634. [4m] T. Komatsu, M. Moritake, E. Tsuchida, *Chem. Eur. J.* **2003**, *9*, 4626−4633. [4n] M.-S. Choi, T. Aida, H. Luo, Y. Araki, O. Ito, *Angew. Chem. Int. Ed.* **2003**, *42*, 4060−4063. [4o] K. Kilså, J. Kajanus, A. Macpherson, J. Mårtensson, B. Albinsson, *J. Am. Chem. Soc.* **2001**, *123*, 3069−3080. [4p] E. Iengo, E. Zangrando, E. Alessio, J.-C. Chambron, V. Heitz, L. Flamigni, J.-P. Sauvage, *Chem. Eur. J.* **2003**, *9*, 5879−5887. [4q] E. K. L. Yeow, K. P. Ghiggino, J. N. H. Reek, M. J. Crossley, A. Bosman, A. P. H. J. Schenning, E. W. Meijer, *J. Phys. Chem. B* **2000**, *104*, 2596−2606. [4r] C. C. Mack, D. Pomeranc, M. Montalti, L. Prodi, J. K. M. Sanders, *Chem. Commun.* **1999**, 1083−1084. [4s] S. Anderson, H. L. Anderson, A. Bashall, M. McPartlin, J. K. M. Sanders, *Angew. Chem.* **1995**, *107*, 1196−1199; *Angew. Chem. Int. Ed. Engl.* **1995**, *34*, 1096−1099.

[5] [5a] H. L. Anderson, *Chem. Commun.* **1999**, 2323−2330. [5b] A. Tsuda, A. Osuka, *Science* **2001**, *293*, 79−82. [5c] I. V. Rubtsov, K. Susumu, G. I. Rubtsov, M. J. Therien, *J. Am. Chem. Soc.* **2003**, *125*, 2687−2696.

[6] N. Solladié, M. Gross, J.-P. Gisselbrecht, C. Sooambar, *Chem. Commun.* **2001**, 2206−2207.

[7] [7a] J. S. Lindsey, I. C. Schreiman, H. C. Hsu, P. C. Kearney, A. M. Marguerettaz, *J. Org. Chem.* **1987**, *52*, 827−836. [7b] J. S. Lindsey, R. W. Wagner, *J. Org. Chem.* **1989**, *54*, 828−836.

[8] Th. Förster, *Discuss. Faraday Soc.* **1959**, *27*, 7−17.

[9] D. L. Dexter, *J. Chem. Phys.* **1953**, *21*, 836−850.

[10] *Hyperchem version 6.02*, Hypercube Inc., Gainesville, Florida, **2000**.

[11] I. Tinoco Jr., *Adv. Chem. Phys.* **1962**, *4*, 113−160.

[12] G. Pescitelli, S. Gabriel, Y. Wang, J. Fleischhauer, R. W. Woody, N. Berova, *J. Am. Chem. Soc.* **2003**, *125*, 7613−7628.
[13] L. Flamigni, A. M. Talarico, B. Ventura, *J. Porphyrins Phthalocyanines* **2003**, 7, 318−327.
[14] [14a] C. A. Hunter, M. N. Meah, J. K. M. Sanders, *J. Am. Chem. Soc.* **1990**, *122*, 5773−5780, [14b] C. C. Mak, N. Bampos, J. K. M. Sanders, *Angew. Chem.* **1998**, *110*, 3169−3172; *Angew. Chem. Int. Ed.* **1998**, *37*, 3020−3023.
[15] J. Brettar, J.-P. Gisselbrecht, M. Gross, N. Solladié, *Chem. Commun.* **2001**, 733−734.
[16] L. Flamigni, *J. Phys. Chem.* **1993**, *97*, 9566−9572.
[17] *Matlab 5.2.,* The MathWorks Inc., Natik Ma 01760, USA.

Received December 10, 2003
Early View Article